

# A NOVEL ELECTRICAL SIGNATURE ANALYSIS (ESA) BASED TECHNIQUE TO IDENTIFY STATOR FAULTS IN BRUSHLESS DC (BLDC) MOTORS

Farhan Ahmed Butt<sup>1</sup>, Dr. Syed Abdul Rehman Kashif<sup>2</sup>

<sup>1,2</sup>Department of Electrical Engineering, University of Engineering and Technology, Lahore, Pakistan.

<sup>1</sup>farhan.ahmed.butt@gmail.com <sup>2</sup>twaseen786@gmail.com

**ABSTRACT** - The paper reports a novel “electrical signature analysis” (ESA) based technique for the detection of stator faults in brushless dc (BLDC) motors. The proposed fault diagnosis methodology is capable of detecting stator phase imbalances and short circuit(s) in windings at incipient stages. To obtain results, “electrical signature analysis” (ESA) is implemented in a real time digital signal processor to execute data acquisition. The comparison and performance evaluation is implemented by observing the spectrum of stator currents under varying load conditions. Experimental measurements agree acceptably with simulation results, and validate the proposed method.

**Key Words:** Brushless DC motor; Electrical Signature Analysis, Data Acquisition.

## 1. INTRODUCTION

BLDC motors are widely used in industrial processes due to their compact size, reduced electro-magnetic interference and constant torque characteristics. Performance monitoring and incipient fault detection of BLDC motors are becoming very important to reduce the machine downtime for unscheduled maintenance, reflecting in less cost and enhanced reliability of the industrial processes. In electro-mechanical devices the most common indication to fault is vibration. Vibrations can be induced into the system due to any stator fault e.g. phase imbalance, inter-turn short circuits and stator winding mismatch. It reduces equipment performance and leads to premature failure. Identifying vibrations at initial stages is one of the main elements of condition monitoring. Which is a more preventive and predictive approach during maintenance and operation of electrical machines.[1]

The basic principal of electrical machines is to convert electrical power to mechanical and vice versa. The machines used in industries often work under varying mechanical stresses. As a result vibrations are induced in the machines. Usually these are measured using vibration analysis techniques which prevail the industry. But sometimes these vibrations are too small to be measured using accelerometers. The vibrations due to faults in the machines and mechanical stresses add up to a signature that may mislead during fault detection in time domain. However, if we use an electrical signature analysis technique and then analyze the spectrum of the stator currents, the time domain misleading phenomena are eliminated.[2,3]

BLDC motors are inside out DC motors having three-phase windings on its stator and a permanent magnet on the rotor. As suggested by its name, the BLDC motors have no brushes resulting in reduced electromagnetic interference and ionizing spikes. Owing to these properties, BLDC motors are used in high performance applications. We need to detect and correct the faults at incipient stages before they escalate into any harmful situation. Many kinds of faults can arise in BLDC motors including stator, rotor, and inverter faults. Rotor and inverter faults are well researched topics as compared to stator faults which are very scarcely researched upon. The research in consideration addresses the stator faults.[4,5]

In this paper, different parameters of BLDC motors are analyzed under different fault conditions. After performing

real time data acquisition, electrical signatures are stored in databases to benchmark different fault conditions. In detail, phase imbalance is observed that can be caused due to inter-turn short circuits, winding mismatch or heating effect.

## 2. BRUSHLESS DC MOTOR DRIVE

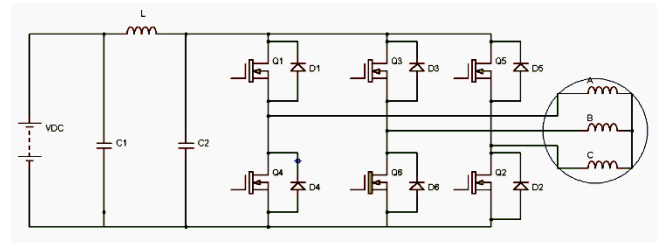


Figure 1: BLDC drive system with motor

A sensed closed loop proportional integral (PI) control algorithm is implemented using dsPIC® digital signal controller. A 24 Volt three-phase permanent magnet BLDC motor is used as shown in the Figure 1. Out of many different control schemes 120° conduction is used to control the MOSFETs. At any time during conduction, only two of the phases are alive. The rotor position is determined via using three Hall Effect sensors that are displaced by 120°. By knowing the position of the rotor we can commute the next pair of stator windings. The speed of the BLDC motor can be controlled by using the potentiometer available on the drive. The PI control algorithm compensates the variations in speed due to varying mechanical stresses on the BLDC motor.[6]

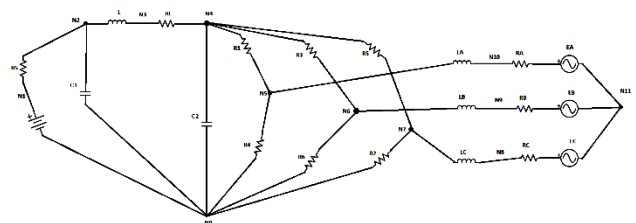


Figure 2: Lumped model of BLDC Drive system

For validation of this proposed technique a discrete time lumped model is implemented for the drive system as shown in Figure 2. [7]

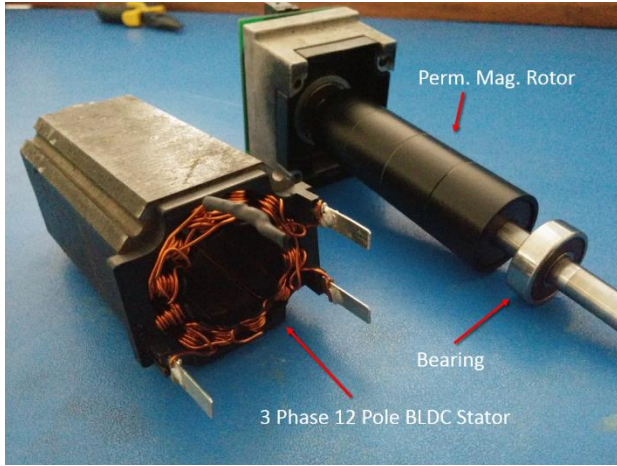


Figure 3: BLDC motor used in the system



Figure 4: Resistance measurement using micro-ohmmeter

An equation set is developed from the discrete time lumped network in equation (1).

$$\begin{bmatrix} U_{rn} \\ U_{gn} \\ U_{bn} \end{bmatrix} = \begin{bmatrix} R_r & 0 & 0 \\ 0 & R_g & 0 \\ 0 & 0 & R_b \end{bmatrix} \begin{bmatrix} i_r \\ i_g \\ i_b \end{bmatrix} + \frac{d}{dt} \begin{bmatrix} L_{rr} & L_{rg} & L_{rb} \\ L_{gr} & L_{gg} & L_{gb} \\ L_{br} & L_{bg} & L_{bb} \end{bmatrix} \begin{bmatrix} i_r \\ i_g \\ i_b \end{bmatrix} + \begin{bmatrix} \frac{d}{dt} \lambda_r \\ \frac{d}{dt} \lambda_g \\ \frac{d}{dt} \lambda_b \end{bmatrix} \quad (1)$$

Where  $U_{an}$ ,  $U_{bn}$  and  $U_{cn}$  are the stator phase voltages;  $R_r$ ,  $R_g$  and  $R_b$  are the stator resistances per phase;  $i_r$ ,  $i_g$  and  $i_b$  are the stator phase currents;  $L_{rr}$ ,  $L_{gg}$  and  $L_{bb}$  are the self-inductances of red, green and black phases respectively;  $L_{rg}$ ,  $L_{gb}$  and  $L_{br}$  are the mutual inductances between red, green and black phases;  $\frac{d}{dt} \lambda_r$ ,  $\frac{d}{dt} \lambda_g$  and  $\frac{d}{dt} \lambda_b$  are the back electromotive forces for the respective phases.

$$\begin{bmatrix} U_{rn} \\ U_{gn} \\ U_{bn} \end{bmatrix} = \begin{bmatrix} R_r i_r \\ R_g i_g \\ R_b i_b \end{bmatrix} + \frac{d}{dt} \begin{bmatrix} L_{rr} i_r + L_{rg} i_g + L_{rb} i_b \\ L_{gr} i_r + L_{gg} i_g + L_{gb} i_b \\ L_{br} i_r + L_{bg} i_g + L_{bb} i_b \end{bmatrix} + \begin{bmatrix} \frac{d}{dt} \lambda_r \\ \frac{d}{dt} \lambda_g \\ \frac{d}{dt} \lambda_b \end{bmatrix} \quad (2)$$

When all the stator currents are balanced i.e.

$$i_r + i_g + i_b = 0 \quad (3)$$

This leads to a simplification of the inductance matrix in equation (2).

$$M i_g + M i_b = -M i_r \quad (4)$$

Where  $M$  is the mutual inductance between phases red, green and black. Equation (1) in state space is now represented as

$$\begin{bmatrix} U_{rn} \\ U_{gn} \\ U_{bn} \end{bmatrix} = \begin{bmatrix} R_r & 0 & 0 \\ 0 & R_g & 0 \\ 0 & 0 & R_b \end{bmatrix} \begin{bmatrix} i_r \\ i_g \\ i_b \end{bmatrix} + \frac{d}{dt} \begin{bmatrix} (L_{rr} - M) i_r & 0 & 0 \\ 0 & (L_{gg} - M) i_g & 0 \\ 0 & 0 & (L_{bb} - M) i_b \end{bmatrix} + \begin{bmatrix} \frac{d}{dt} \lambda_r \\ \frac{d}{dt} \lambda_g \\ \frac{d}{dt} \lambda_b \end{bmatrix} \quad (5)$$

During the fault on red phase  $R_r \neq (R_g = R_b = R_{st})$  condition occurs. Rotor is in such a position that the current is going into red and out of green phase.

$$V_{rg} = v_{rn} - v_{gn} = i_r (R_r + R_g) + i_r \left( \frac{d}{dt} L_{rr} - 2 \frac{d}{dt} i_{rg} + \frac{d}{dt} L_{gg} \right) + \frac{d}{dt} i_r (L_{rr} - 2L_{rg} + L_{gg}) + \frac{d}{dt} \lambda_r' - \frac{d}{dt} \lambda_g' \quad (6)$$

Where  $\frac{d}{dt} \lambda_r'$  and  $\frac{d}{dt} \lambda_g'$  are the derivatives of the flux linkages (back electromotive forces) when phase imbalance occurs on the stator winding.

During the fault on black phase  $R_b \neq (R_r = R_g = R_{st})$  condition occurs. Rotor is in such a position that the current is going into black and out of green phase.

$$V_{bg} = v_{bn} - v_{gn} = i_b (R_b + R_g) + i_b \left( \frac{d}{dt} L_{bb} - 2 \frac{d}{dt} i_{bg} + \frac{d}{dt} L_{gg} \right) + \frac{d}{dt} i_b (L_{bb} - 2L_{bg} + L_{gg}) + \frac{d}{dt} \lambda_b' - \frac{d}{dt} \lambda_g' \quad (7)$$

Where  $\frac{d}{dt} \lambda_r'$  and  $\frac{d}{dt} \lambda_g'$  are the derivatives of the flux linkages (back electromotive forces) when a phase imbalance occurs on the stator winding.

### 3. METHODOLOGY: LABORATORY SETUP

To validate the results practically in laboratory environment a three-phase, 12-pole permanent magnet motor is used with dsPIC® controller. The revolutions per minute (rpm) of the BLDC motor can be controlled by the potentiometer available on the drive circuit. A Hall Effect sensor is used to get the signatures of the stator current, which is then processed through a data acquisition (DAQ) device. To simulate the varying load condition on BLDC motor in lab environment a Direct Current series generator is used. By varying the electrical loading on DC generator varying mechanical stresses are produced. All the waveforms are then saved to benchmark the fault conditions. The complete laboratory setup is shown in Figure 5.

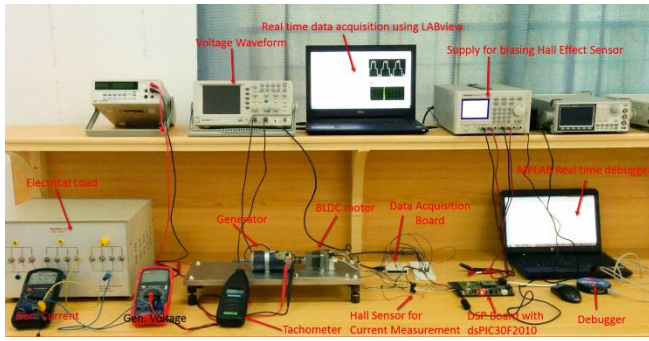


Figure 5: Experimental Setup in Laboratory Environment

4. RESULTS: FAULT IDENTIFICATION

A Hall Effect sensor is used to get the signature of all the stator currents. Real time Fourier analysis is then performed on this electrical signatures of the signals and the results are stored in databases during healthy and faulty operating conditions. Figure 6 shows the healthy signatures of the BLDC motor.

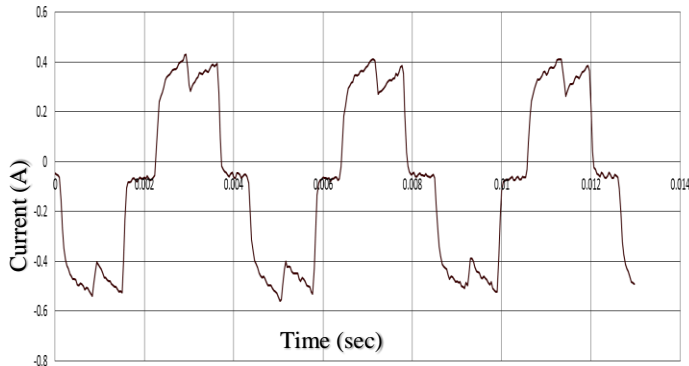


Figure 6: Healthy Signature of BLDC motor

From the spectrum of the Figure 6, it is clear that there is no 3<sup>rd</sup> harmonic present in the stator current spectrum. A slight bump at 709 Hz (3<sup>rd</sup> harmonics) is due to the difference in electrical resistance between the stator windings that are confirmed by micro-ohm meter equipment as shown in Figure 4.

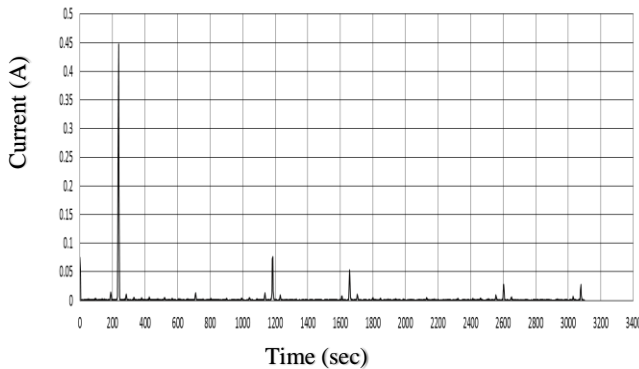


Figure 7: Current Spectrum during healthy condition

From the database of the healthy signatures of BLDC motor Table 1 is constructed and then all the harmonics are

normalized with respect to the fundamental harmonic. Ideally speaking, there should have been no 3<sup>rd</sup> harmonic in the current spectrum of the waveform during healthy operating condition, but due to difference in the electrical resistance of the windings a small value appears in the signature.

Table 1: Harmonic Levels during Healthy Conditions

Harmonic #	Harmonic Value
$f_1$	0.4470356
$f_3$	0.0132058 (2%)
$f_5$	0.0754786 (17%)
$f_7$	0.0528861 (12%)
$f_9$	0.0030561 (0.5%)
$f_{11}$	0.0273015 (6.1%)

Total harmonic distortion calculated using Table 1 is given as  $THD_i$

$$THD_i = \frac{\sqrt{\sum_{h=2}^{h_{max}} i_h^2}}{i_1} = 21.6\% \quad (8)$$

When the mechanical loading is provided to BLDC motor using DC series generator, it depicts an increase in THD as confirmed by equation (3) and (4). THD is increased from 21.6% to 25.6%.

$$THD_i = \frac{\sqrt{\sum_{h=2}^{h_{max}} i_h^2}}{i_1} = 25.6\% \quad (9)$$

Figure 8 shows the two overlapped waveforms during healthy and faulty operating conditions. The frequency of operation observed during fault condition is lesser than during healthy conditions. It is due to the fact that by increasing the stator resistance the angular frequency  $\omega_r$  decreases.

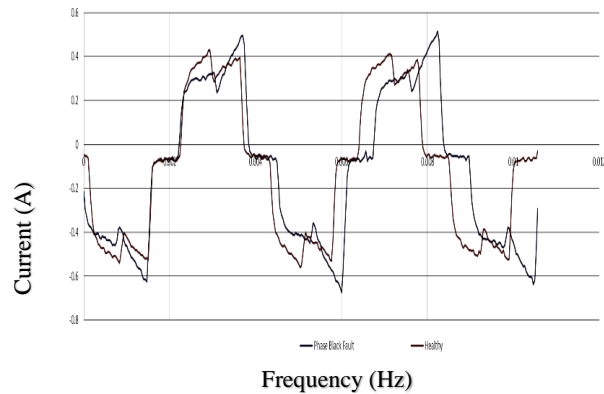


Figure 8: Faulty Signature of BLDC motor

Harmonics obtained during the fault at black phase are shown in Figure 9 confirms the presence of 3<sup>rd</sup> harmonics in the spectrum.

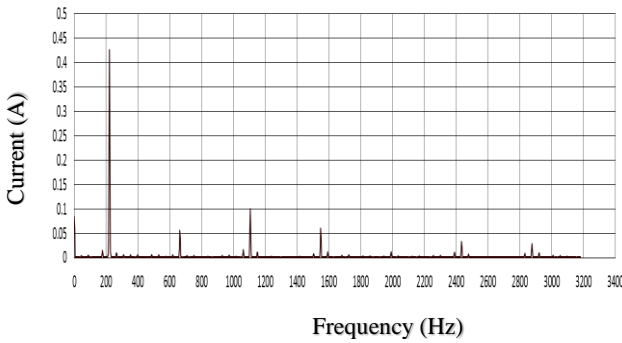


Figure 9: Current Spectrum during faulty condition

Table 2 shows the critical analysis of the normalized harmonic values during healthy and faulty operating environments. During faulty operation triplen harmonics are escalated into the system and the total harmonic distortion is increased to 31.3% as compared to 21.7%. 3<sup>rd</sup> and 9<sup>th</sup> harmonic has been observed almost 6 to 7 times more in value than at healthy condition.

Table 2: Harmonics values during Phase imbalance

Harmonic #	Harmonics During phase Imbalance
$f_1$	0.4255066
$f_3$	0.0551565 (13%)
$f_5$	0.099899 (23.4%)
$f_7$	0.0593031 (14%)
$f_9$	0.0114581 (3%)
$f_{11}$	0.0327101 (8%)

$$THD_i = \frac{\sqrt{\sum_{h=2}^{h_{max}} i_h^2}}{i_1} = 31.2\% \quad (5\%)$$

5. DISCUSSION

Table 3: Comparative study of Harmonics at Healthy and Faulty condition

Harmonic #	Harmonics During phase Imbalance	Healthy Harmonic condition
$f_1$	0.4255066	0.4470356
$f_3$	0.0551565 (13%)	0.0132058 (2%)
$f_5$	0.099899 (23.4%)	0.0754786 (17%)
$f_7$	0.0593031 (14%)	0.0528861 (12%)
$f_9$	0.0114581 (3%)	0.003056 (0.5%)
$f_{11}$	0.0327101 (8%)	0.027301 (6.1%)

Table-3 summarizes the results presented for harmonic analysis. When the mechanical loading is provided to BLDC motor using DC series generator, it confirms an increase in THD. Also the 3<sup>rd</sup> harmonic level jumps from 2% to 13%, almost 7 times the value as in healthy condition. 9<sup>th</sup> harmonic is 3% in value during faulty condition which is also 6 times more in value. The comparative study shows that triplen harmics are negligible during healthy operating conditions but they escalate into the system as the fault occurs.

6. CONCLUSION

Although accelarometers based techniques which measure vibrations in the system as an indication to the fault condition are considered to be more reliable in industrial processes but they can not provide any information about the electrical parameters inside the BLDC motors. Due to the cost effective nature of electrical signature analysis technique as compared to the vibration analysis, ESA is preffered. It provides us the information about the electrical characteristics inside the BLDC motor. Also noise in the time domain signals that can mislead us, when converted to frequency domain, it possesses a certain pattern and information which is useful during fault identification. It is clear from the experimental results that when the stator of BLDC motor is subjected to a fault triplen harmonics appears in the power system, which could be observed by the spectrum of the stator currents.

7. REFERENCES

- [1]. Rajagopalan S, Aller, J.M, Restrepo J.A, Habetler T.G, Harley R.G, "Detection of Rotor Faults in Brushless DC Motors Operating Under Nonstationary Conditions," *Industry Applications, IEEE Trans. on Industry Applications*, vol. 42, pp. 1464 – 1477, Nov.-dec. 2006C.
- [2]. Taeyong Yoon, "Magnetically induced vibration in a permanent-magnet brushless DC motor with symmetric pole-slot configuration," *IEEE Trans. on Magnetics*, vol. 41, pp. 2173 – 2179, June 2005
- [3]. Li Jianjun, Xu Yongxiang and Zou Jibin, "A study on the reduction of vibration and acoustic noise for brushless DC motor," *In Electrical Machines and Systems*, 2008. ICEMS 2008. *International Conference on*, Oct. 2008, pp. 561 – 563
- [4]. S. Rajagopalan, T. G. Habetler, R. G. Harley, T. Sebastian and B. Lequesne, "Current/Voltage Based Detection of Faultsin Gears Coupled to Electric Motors," *IEEE Trans. on Industry Applications*, vol. 42, pp. 1412 – 1420, Nov.-dec. 2006
- [5]. Satish Rajagopalan, Wiehan le Roux, Thomas G. Habetler, and Ronald G. Harley, "Dynamic eccentricity and demagnetized rotor magnet detection in trapezoidal flux (brushless dc) motors operating under different load conditions," *IEEE Trans. On Power Electronics*, vol. 22, pp. 2061 – 2069, Sept. 2007
- [6]. Zubizarreta-Rodriguez, J.F.; Vasudevan, S. "Condition monitoring of brushless DC motors with non-stationary dynamic conditions", *Instrumentation and Measurement Technology Conference (I2MTC) Proceedings*, 2014 IEEE International, On page(s): 62 - 67
- [7]. Mohamed A. Awadallah, M. Morcos, Suresh Gopalakrishnan, and Thomas W. Nehl, " Detection of Stator Short Circuits in VSI-Fed Brushless DC Motors Using Wavelet Transform," *IEEE Trans. On ENERGY CONVERSION*, vol. 21, pp. 1 – 8, March 2006